Modulational instability of zone boundary mode in nonlinear lattices: Rigorous results

Kazuyuki Yoshimura*
NTT Communication Science Laboratories, NTT Corporation, 2-4 Hikaridai, Seika-cho, Soraku-gun, Kyoto 619-0237, Japan
(Received 13 February 2004; published 27 July 2004)

We study the modulational instability of the zone boundary mode in nonlinear lattices with generic polynomial potentials. We present an exact expression of the instability growth rate in the high energy limit. The unstable wave number range and the most unstable wave number are obtained. Relevance of the present results on an energy localization state, which appears after growth of the modulational instability, is also discussed.

DOI: 10.1103/PhysRevE.70.016611 PACS number(s): 05.45.−a

I. INTRODUCTION

Fermi, Pasta, and Ulam (FPU) were the first to study the relaxation to equilibrium of one-dimensional nonlinear lattices [1]. They numerically integrated the equations of motion with an initial condition far from equilibrium, giving all energy to the lowest wave number normal mode. It is well known that they observed the recurrence phenomenon instead of the relaxation to the equilibrium state. For historical reasons, the relaxation toward equilibrium has been usually studied with an initial condition where a small number of low wave number modes were excited. Recently, several works have been devoted to the relaxation from an initial excitation of the *zone boundary mode* (ZBM), which is the highest wave number mode [2–4]. These investigations demonstrated that localized modes called *discrete breathers or intrinsic localized modes*, which were discovered by Takeno *et al.* [5], emerge and play an important role in the relaxation process. In addition, it was shown in Ref. [6] that the discrete breathers emerge also from an initial excitation of a high wave number mode other than the ZBM.

The modulational instability is the fundamental mechanism for spontaneous generation of the discrete breathers out of a small initial perturbation on the initially excited mode. It is important to clarify the nature of the modulational instability for better understanding of the discrete breather generation and the relaxation process in nonlinear lattices. The modulational instability is studied for the FPU lattice [4,7–14] and the nonlinear Klein-Gordon lattice [15,16]. The modulational instability of an arbitrary wave number mode is studied in Refs. [12,15,16] while that of the ZBM is studied in the other references. In Ref. [14], stability of some other low-dimensional invariant subsets of modes is also studied for the FPU lattice besides that of the ZBM. However, these works are numerical or approximate analytical analyses and no rigorous result on the modulational instability has yet been obtained. In the present paper, we study the modulational instability in nonlinear lattices with generic polynomial potentials and present exact results on the instability growth rate in the high energy limit.

The present paper is organized as follows. In Sec. II, we describe a correspondence between the variational equation of a homogeneous potential system and the Gauss hypergeometric equation and then review some known results on a monodromy matrix of the Gauss hypergeometric equation. In Sec. III, we describe the nonlinear lattice model, the normal mode coordinates, and the ZBM solution. In Sec. IV, we calculate the instability growth rate in the high energy limit. Moreover, we discuss relevance of the present results on the energy localization state consisting of the discrete breathers, which appears after growth of the modulational instability. Conclusions are offered in Sec. V.

II. GAUSS HYPERGEOMETRIC EQUATION AND MONODROMY MATRIX

Consider the linear differential equation

$$\frac{d^2y}{dt^2} + g(t)y = 0, \tag{1}$$

where $g(t)$ is a periodic function with the period T. Let $\{y_1, y_2\}$ be a system of fundamental solutions of Eq. (1). According to the Floquet theory, solutions of Eq. (1) at $t=t$ and $t+T$ are related via a 2×2 *monodromy matrix* $\boldsymbol{M}$ as

$$(y_1(t+T), y_2(t+T)) = (y_1(t), y_2(t)) \cdot \boldsymbol{M}. \tag{2}$$

The eigenvalues of $\boldsymbol{M}$ are called the *characteristic multipliers* and given in the form $\{\rho, \rho^{-1}\}$ because of $\boldsymbol{M} \in \mathrm{SL}(2,\mathbf{C})$. The *characteristic exponents* are defined by $\sigma = \pm T^{-1}\ln|\rho|$. Equation (1) has unstable solutions if there is a positive σ.

The monodromy matrix $\boldsymbol{M}$ can be analytically calculated in some particular cases although the calculation is impossible in general. One of such cases is the case of a homogeneous potential system. We review some known results on the monodromy matrix for the homogeneous potential system [17,18]. Consider the set of equations

$$\frac{d^2\varphi}{dt^2} + \alpha_{2m}\varphi^{2m-1} = 0 \tag{3}$$

and

$$\frac{d^2\xi}{dt^2} + \beta_{2m}\varphi(t)^{2m-2}\xi = 0, \tag{4}$$

where m is a positive integer, α_{2m} and β_{2m} are real constants, and we assume $\alpha_{2m} > 0$. We define a parameter λ_{2m} as

$$\lambda_{2m} = \frac{\beta_{2m}}{\alpha_{2m}}, \tag{5}$$

*Email address: kazuyuki@cslab.kecl.ntt.co.jp

which we call the *stability parameter*. Equation (3) has the integral

$$\frac{1}{2}\left(\frac{d\varphi}{dt}\right)^2 + \frac{\alpha_{2m}}{2m}\varphi^{2m} = h, \qquad (6)$$

where $h \in \mathbf{R}$ is a constant corresponding the energy. The left hand side of Eq. (6) can be regarded as the Hamiltonian of a nonlinear oscillator with the homogeneous potential of the order $2m$. From Eq. (6), a periodic solution $\varphi(t)$ of Eq. (3) is determined as the inverse function of the integral

$$t = \int_{\varphi_0}^{\varphi} dw/\sqrt{P(w)}, \qquad (7)$$

with

$$P(w) = 2\left[h - \left(\frac{\alpha_{2m}}{2m}\right)w^{2m}\right], \qquad (8)$$

where φ_0 is a constant corresponding to the initial condition, i.e., $\varphi(0)=\varphi_0$. If we consider integral (7) in the complex domain, then there exist branch points $\hat{s}_k$ of the Riemann surface defined by $z=\sqrt{P(w)}$, which are located at

$$\hat{s}_k = \left(\frac{2mh}{\alpha_{2m}}\right)^{1/2m}\exp\left[i\frac{\pi k}{m}\right], \quad k = 0,1,\ldots,2m-1. \qquad (9)$$

Two points $\hat{s}_0=(2mh/\alpha_{2m})^{1/2m}$ and $\hat{s}_m=-(2mh/\alpha_{2m})^{1/2m}$ are on the real axis. Let γ be a counterclockwise circuit encircling these two branch points $\hat{s}_0$ and $\hat{s}_m$ in the complex w plane. The real period of solution $\varphi(t)$ is given by the integral

$$T_{hom} = \oint_{\gamma} dw/\sqrt{p(w)}. \qquad (10)$$

The monodromy matrix $\boldsymbol{M}$ for the real period is determined from analytical continuation of a system of fundamental solutions of Eq. (4) along γ.

It is shown in Ref. [17] that Eq. (4) is transformed into the Gauss hypergeometric equation by the change of the independent variable from t to $z=\{\varphi(t)\}^{2m}$. This fact enables us to obtain an explicit expression for the monodromy matrix $\boldsymbol{M}$ of Eq. (4) corresponding to the real period. If we make this change of variable in Eq. (4) then we have

$$z(1-z)\frac{d^2\xi}{dz^2} + [c-(a+b+1)z]\frac{d\xi}{dz} - ab\xi = 0, \qquad (11)$$

where

$$a+b = \frac{1}{2} - \frac{1}{2m}, \quad ab = -\frac{\lambda_{2m}}{4m}, \quad c = 1 - \frac{1}{2m}. \qquad (12)$$

Equation (11) has two singular points at $z=0$ and 1 in the finite z plane. Let γ_0 and γ_1 be counterclockwise circuits encircling $z=0$ and $z=1$ with a common base point z_0 on the real axis $(0<z_0<1)$, respectively. Explicit expressions of the monodromy matrices of Eq. (11) corresponding to γ_0 and γ_1, which we denote by $\boldsymbol{M}(\gamma_0)$ and $\boldsymbol{M}(\gamma_1)$, respectively, are known (e.g., Ref. [19]). The path γ in the w plane is mapped into $\gamma_1\gamma_0^m\gamma_1\gamma_0^m$ in the z plane by the mapping $z=w^{2m}$, where $\gamma_1\gamma_0^m\gamma_1\gamma_0^m$ stands for the circuit consisting of γ_1, γ_0^m, γ_1, and γ_0^m in this order. Therefore the monodromy matrix $\boldsymbol{M}$ can be obtained by the product $\boldsymbol{M}(\gamma_1)\boldsymbol{M}(\gamma_0)^m\boldsymbol{M}(\gamma_1)\boldsymbol{M}(\gamma_0)^m$ for a certain system of fundamental solutions. After some calculation, we can obtain the explicit expression of $\boldsymbol{M}$ as follows (for details, see Ref. [17]):

$$\boldsymbol{M} = \begin{pmatrix} -1 & -BC \\ A & ABC-1 \end{pmatrix}^2, \qquad (13)$$

where

$$A = 1 - e^{-i\pi(2a+1/m)}, \quad B = 1 - e^{-i\pi(2b+1/m)}, \quad C = 2/(1-e^{-i\pi/m}). \qquad (14)$$

A simple computation shows that

$$\mathrm{tr}\boldsymbol{M} = 2F_{2m}(\lambda_{2m}), \qquad (15)$$

where

$$F_{2m}(\lambda_{2m}) = \frac{2}{\sin^2(\pi/2m)}\cos^2\left[\frac{\pi}{2m}\sqrt{(m-1)^2+4m\lambda_{2m}}\right] - 1. \qquad (16)$$

The eigenvalues $\{\rho_{hom},\rho_{hom}^{-1}\}$ of $\boldsymbol{M}$ can be obtained from the equation $\rho^2-(\mathrm{tr}\,\boldsymbol{M})\rho+1=0$. Solving this equation and using the definition $\sigma_{hom}=\pm T_{hom}^{-1}\ln|\rho_{hom}|$, we can obtain the characteristic exponents as follows:

$$\sigma_{hom} = \pm\frac{1}{T_{hom}}\ln\left|F_{2m}(\lambda_{2m}) + \sqrt{\{F_{2m}(\lambda_{2m})\}^2-1}\right|. \qquad (17)$$

This shows that there is a positive characteristic exponent if and only if $F_{2m}(\lambda_{2m})>1(\mathrm{tr}\boldsymbol{M}>2)$. It can be easily shown that $F_{2m}(\lambda_{2m})>1$ holds when λ_{2m} is in the region S_{2m} defined by

$$S_{2m} = \{\lambda\in\mathbf{R}|\lambda<0, 1<\lambda<2m-1, 2m+2<\lambda<6m-2,\ldots,j(j-1)m+j<\lambda<j(j+1)m-j,\ldots\}. \qquad (18)$$

III. NONLINEAR LATTICE AND ZBM

Our investigation is of the nonlinear lattice model described by the Hamiltonian

$$H = \frac{1}{2}\sum_{i=1}^{N} p_i^2 + \sum_{i=1}^{N}[U(q_i) + V(q_i - q_{i-1})] \qquad (19)$$

with the periodic boundary condition, i.e., $q_0=q_N$. The on-site potential U and the nearest neighbor interaction potential V are of the forms

$$U(X) = \sum_{r=1}^{m} \frac{\mu_{2r}}{2r} X^{2r}, \; V(X) = \sum_{r=1}^{m} \frac{\kappa_{2r}}{2r} X^{2r}, \tag{20}$$

where $\mu_{2r} \in \mathbf{R}$ and $\kappa_{2r} \in \mathbf{R}$ are the constants. We assume that $\mu_{2m} \geqslant 0$ and $\kappa_{2m} > 0$. The equations of motion derived from the Hamiltonian (19) are

$$\frac{d^2 q_i}{dt^2} + \sum_{r=1}^{m} [\mu_{2r} q_i^{2r-1} + \kappa_{2r}\{(q_i - q_{i-1})^{2r-1} + (q_i - q_{i+1})^{2r-1}\}] = 0, \tag{21}$$

where $i = 1, 2, \ldots, N$.

The transformation $\boldsymbol{q} = (q_1, \ldots, q_N) \mapsto \boldsymbol{Q} = (Q_0, \ldots, Q_{N-1})$ defined by

$$q_i = \frac{1}{\sqrt{N}} \sum_{k=0}^{N-1} Q_k \left[\sin\left(\frac{2\pi k}{N} i\right) + \cos\left(\frac{2\pi k}{N} i\right) \right], \quad i = 1, 2, \ldots, N, \tag{22}$$

gives the normal modes of the corresponding linear system. Here, Q_k is the amplitude of kth normal mode. The conjugate momentum P_k is defined by $P_k = \dot{Q}_k$. The ZBM is the normal mode of $k = N/2$, which corresponds to the displacement pattern $q_i = (-1)^i Q_{N/2} / \sqrt{N}$. It is easy to check that Eq. (21) has a particular solution of the form $q_i(t) = (-1)^i \varphi(t)$. Thus the ZBM of the corresponding linear system still gives an exact periodic solution for the nonlinear lattice (19). By the substitution $q_i(t) = (-1)^i \varphi(t)$ in Eq. (22), we have the equation for $\varphi(t)$ as

$$\frac{d^2 \varphi}{dt^2} + \sum_{r=1}^{m} (\mu_{2r} + 2^{2r} \kappa_{2r}) \varphi^{2r-1} = 0, \tag{23}$$

with the integral

$$\frac{1}{2} \left(\frac{d\varphi}{dt} \right)^2 + \sum_{r=1}^{m} \frac{1}{2r} (\mu_{2r} + 2^{2r} \kappa_{2r}) \varphi^{2r} = h, \tag{24}$$

where $h \in \mathbf{R}$ is the energy density defined by $h = E/N$, where E is the total energy of the lattice. Using this integral, the solution $\varphi(t)$ is obtained in the form (7) with

$$P(w) = 2\left[h - \sum_{r=1}^{m} \frac{1}{2r} (\mu_{2r} + 2^{2r} \kappa_{2r}) w^{2r} \right]. \tag{25}$$

Let $s_k(h), k = 0, 1, \ldots, 2m-1$ be solutions of the algebraic equation $P(w) = 0$. They are the branch points of the Riemann surface defined by $z = \sqrt{P(w)}$. Since $\mu_{2m} + 2^{2m} \kappa_{2m} > 0$, there exist two real branch points $s_0(h)$ and $s_m(h)$ for $h > h_0$, where h_0 is a sufficiently large positive constant. We define a counterclockwise circuit Γ encircling these two real branch points. The real period $T(h)$ of $\varphi(t)$ is given by

$$T(h) = \oint_\Gamma dw / \sqrt{P(w)}. \tag{26}$$

We note that the period $T(h)$ depends on h.

IV. STABILITY ANALYSIS OF ZBM

Let us consider the variational equations along the ZBM solution. Linearizing Eq. (21), we can obtain the variational equations in the vector form

$$\frac{d^2 \boldsymbol{\xi}}{dt^2} + \left[\left\{ \sum_{r=1}^{m} (2r-1) \mu_{2r} \varphi(t)^{2r-2} \right\} \cdot \boldsymbol{I} + \left\{ \sum_{r=1}^{m} (2r-1) \kappa_{2r} (2\varphi(t))^{2r-2} \right\} \cdot \boldsymbol{A} \right] \cdot \boldsymbol{\xi} = 0, \tag{27}$$

where $\boldsymbol{\xi} = (\xi_1, \ldots, \xi_N)$ and each $\xi_i, i = 1, \ldots, N$ represents the variation in q_i. In Eq. (27), $\boldsymbol{I}$ is the $N \times N$ identity matrix and $\boldsymbol{A}$ is the $N \times N$ matrix defined by

$$\boldsymbol{A} = \begin{pmatrix} 2 & -1 & & & -1 \\ -1 & 2 & -1 & & \\ & \ddots & \ddots & \ddots & \\ & & -1 & 2 & -1 \\ -1 & & & -1 & 2 \end{pmatrix}, \tag{28}$$

where the vanishing components are zero. To obtain the decoupled form of the variational equations, we introduce new variables η_k defined by

$$\xi_i = \frac{1}{\sqrt{N}} \sum_{k=0}^{N-1} \eta_k \left[\sin\left(\frac{2\pi k}{N} i\right) + \cos\left(\frac{2\pi k}{N} i\right) \right], \quad i = 1, 2, \ldots, N. \tag{29}$$

The variable η_k is the variation in the kth normal mode coordinate Q_k. If we change variables from ξ_i to η_k, Eq. (27) is rewritten in the form

$$\frac{d^2 \eta_k}{dt^2} + \left[\sum_{r=1}^{m} (2r-1)(\mu_{2r} + 2^{2r-2} \omega_k^2 \kappa_{2r}) \varphi(t)^{2r-2} \right] \eta_k = 0, \quad k = 0, 1, \ldots, N-1, \tag{30}$$

where $\omega_k^2, k = 0, 1, \ldots, N-1$ are the eigenvalues of $\boldsymbol{A}$ and given by

$$\omega_k^2 = 4 \sin^2\left(\frac{\pi k}{N}\right). \tag{31}$$

The monodromy matrix of Eq. (30) for the real period is determined from analytical continuation of a system of fundamental solutions of Eq. (30) along Γ.

We consider Eq. (30) with Eq. (23) in the limit $h \to \infty$. As pointed out in Ref. [18], in this limit, the highest order terms become dominant in Eqs. (23) and (30). Thus the monodromy matrix for the real period of Eq. (30) converges to that of the equation

$$\frac{d^2\eta_k}{dt^2} + (2m-1)(\mu_{2m} + 2^{2m-2}\omega_k^2\kappa_{2m})\varphi(t)^{2m-2}\eta_k = 0, \tag{32}$$

with

$$\frac{d^2\varphi}{dt^2} + (\mu_{2m} + 2^{2m}\kappa_{2m})\varphi^{2m-1} = 0, \tag{33}$$

for which we can calculate an explicit expression of the monodromy matrix. This fact can be confirmed by making the change of scale $\varphi \to h^{1/2m}\varphi, t \to h^{(1-m)/2m}t$, in Eqs. (23) and (30). From Eqs. (32) and (33), the stability parameter for the kth variational equation reads

$$\lambda_{2m}(k) = (2m-1)\frac{\theta_{2m} + \sin^2(\pi k/N)}{\theta_{2m} + 1}, \tag{34}$$

where

$$\theta_{2m} = \frac{\mu_{2m}}{2^{2m}\kappa_{2m}}. \tag{35}$$

Let $\{\rho_{hom}, \rho_{hom}^{-1}\}$ be the characteristic multipliers of the monodromy matrix of Eq. (32), where we assume $|\rho_{hom}| \geqslant 1 \geqslant |\rho_{hom}^{-1}|$. We can obtain ρ_{hom} as

$$\rho_{hom} = F_{2m}(\lambda_{2m}(k)) + \sqrt{\{F_{2m}(\lambda_{2m}(k))\}^2 - 1}, \tag{36}$$

where F_{2m} is the function defined by Eq. (16). It should be noted that ρ_{hom} depends on k but not on h.

Let denote one of the characteristic multipliers of Eq. (30) by $\rho(h)$ and assume $|\rho(h)| \geqslant 1$. The characteristic multiplier $\rho(h)$ converges to ρ_{hom} in the limit $h \to \infty$: i.e., $\rho(h)$ is of the form $\rho(h) = \rho_{hom} + \varepsilon(h)$, where $\varepsilon(h)$ is a function such that $\varepsilon(h) \to 0$ for $h \to \infty$. The exponential growth rate $\sigma(k,h)$ of the solution η_k of Eq. (30) is a function of k and h and given by $\sigma(k,h) = T(h)^{-1}\ln|\rho(h)|$. Thus we can obtain $\sigma(k,h)$ as follows:

$$\sigma(k,h) = \frac{1}{T(h)}\ln\left|F_{2m}(\lambda_{2m}(k)) + \sqrt{\{F_{2m}(\lambda_{2m}(k))\}^2 - 1} + \varepsilon(h)\right|, \tag{37}$$

where $T(h)$ is the period given by Eq. (26). Equation (37) indicates that the h dependence of $\sigma(k,h)$ is essentially determined by that of $T(h)$ for large h. If we make the change of variable $w = h^{1/2m}w'$ in Eq. (26), then we have

$$T(h) \simeq h^{-(1/2-1/2m)}\oint_{\Gamma'} dw'/\sqrt{2\{1 - [(\mu_{2m} + 2^{2m}\kappa_{2m})/2m]w'^{2m}\}} \tag{38}$$

for large h, where Γ' is a counterclockwise circuit encircling the two real branch points $w' = \pm\{2m/(\mu_{2m} + 2^{2m}\kappa_{2m})\}^{1/2m}$. Since the integral in Eq. (38) is independent of h, we can find the scaling law of $T(h) \sim h^{-(1/2-1/2m)}$ for large h. Therefore the scaling law for the exponential growth rate $\sigma(k,h)$ is

$$\sigma(k,h) \sim h^{1/2-1/2m} \tag{39}$$

in the high energy density region. This scaling law is also found in Refs. [10,11] based on an approximate analysis.

Let us consider the k dependence of the exponential growth rate in the limit $h \to \infty$. Since there exists the maximal value $\max_k\sigma(k,h)$ of $\sigma(k,h)$ for fixed h, we can define a normalized exponential growth rate by

$$\begin{aligned}\tilde{\sigma}(k) &= \lim_{h\to\infty}\frac{\sigma(k,h)}{\max_k\sigma(k,h)}\\ &= C_0\ln\left|F_{2m}(\lambda_{2m}(k)) + \sqrt{\{F_{2m}(\lambda_{2m}(k))\}^2 - 1}\right|,\end{aligned} \tag{40}$$

where we regard k as a continuous parameter in the range $k \in [0, N-1]$ and C_0 is a constant such that the maximal value of $\tilde{\sigma}(k)$ may be unity. The k dependence of the exponential growth rate given by Eq. (40) is exact in the limit $h \to \infty$.

We proceed to determine a range of k for unstable perturbations. Equation (40) indicates that $\tilde{\sigma}(k) > 0$ if and only if $F_{2m}(\lambda_{2m}(k)) > 1$. As mentioned in Sec. II, $F_{2m}(\lambda_{2m}(k)) > 1$ is equivalent to the condition that $\lambda_{2m}(k)$ is in the region S_{2m} defined by Eq. (18). It follows from Eq. (34) that $0 \leqslant \lambda_{2m}(k) \leqslant 2m-1$ when $\theta_{2m} \geqslant 0$. Therefore, we have the condition $1 < \lambda_{2m}(k) < 2m-1$ for the unstable perturbations. Using this condition and Eq. (34), we can determine a critical wave number k_c such that perturbations for $k_c < k < N-k_c$ $(k \neq N/2)$ are unstable as follows:

$$k_c = \frac{N}{\pi}\arcsin\left[\sqrt{\frac{1}{2m-1} - \frac{2(m-1)}{2m-1}\theta_{2m}}\right]. \tag{41}$$

If the term inside the root sign is negative, i.e., $\theta_{2m} > 1/2(m-1)$, then perturbations of any wave number are unstable. Equation (41) shows that k_c decreases with increasing θ_{2m}. That is, the unstable wave number range extends as the contribution of the on-site potential U relative to V becomes large. When θ_{2m} exceeds the threshold value $1/2(m-1)$, all wave numbers are in the unstable range. Let us consider the case of $\theta_{2m} = 0$, i.e., $\mu_{2m} = 0$. For this case, we have $k_c = (N/\pi)\arcsin[1/\sqrt{2m-1}]$. This indicates that the unstable wave number range extends and k_c approaches zero as the order of the potential increases. In a particular case of $m=2$, which corresponds to the FPU-β lattice, we have $k_c = (N/\pi)\arcsin[1/\sqrt{3}] \simeq 0.196N$ and this result coincides with an estimation obtained in Refs. [9,11].

Using Eq. (40) we determine the most unstable wave number $k_{max} \in [0, N/2)$, which has the largest exponential growth rate. Equation (40) indicates that $\tilde{\sigma}(k)$ is a monotonous increasing function of F_{2m} when $F_{2m} > 1$. It follows that $(2m-1)/(1+\theta_{2m}^{-1}) \leqslant \lambda_{2m}(k) \leqslant 2m-1$ from Eq. (34). Therefore, we can obtain k_{max} by determining the value λ^* of λ that maximizes $F_{2m}(\lambda)$ in the range $\max\{1, (2m-1)/(1+\theta_{2m}^{-1})\} \leqslant \lambda \leqslant 2m-1$ and then solving the equation $\lambda_{2m}(k) = \lambda^*$ with respect to k. The k_{max} is obtained as follows:

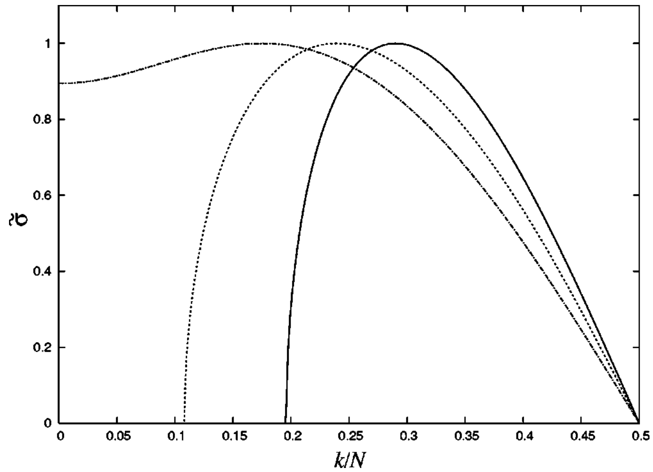

FIG. 1. Examples of $\tilde{\sigma}$ plotted against k/N for three cases: $m=2, \theta_{2m}=0$ (solid line), $m=5, \theta_{2m}=0$ (dashed line), and $m=2, \theta_{2m}=15$ (dash-dotted line).

$$k_{max} = \begin{cases} \frac{N}{\pi}\arcsin\left[\sqrt{\frac{3m^2+2m-1}{4m(2m-1)} - \frac{5m^2-6m+1}{4m(2m-1)}\theta_{2m}}\right] \\ \text{if} \quad \theta_{2m} < \frac{3m^2+2m-1}{5m^2-6m+1}, \\ 0 \\ \text{if} \quad \theta_{2m} \geqslant \frac{3m^2+2m-1}{5m^2-6m+1}. \end{cases} \tag{42}$$

Equation (42) shows that k_{max} decreases as θ_{2m} increases, in other words, as the contribution of U relative to V increases. In addition, Eq. (42) shows that the $k=0$ mode, the translational mode, becomes most unstable when θ_{2m} is not less than the threshold value $(3m^2+2m-1)/(5m^2-6m+1)$. For the case $\theta_{2m}=0$, we have

$$k_{max} = (N/\pi)\arcsin[\sqrt{(3m^2+2m-1)/4m(2m-1)}].$$

Thus the most unstable wave number k_{max} converges to $(N/\pi)\arcsin[\sqrt{3/8}] \simeq 0.210N$ in the limit $m \to \infty$. If we consider the case $m=2$, we have $k_{max}=(N/\pi)\arcsin[\sqrt{5/8}] \simeq 0.290N$. A close estimation $k_{max}=(N/\pi)\arcsin[\sqrt{8/\sqrt{3}-4}] \simeq 0.288N$ has been obtained in Refs. [10,11].

Some examples of $\tilde{\sigma}$ plotted against k/N are shown in Fig. 1. These examples are plotted only for $0 \leqslant k/N \leqslant 1/2$ since the function $\tilde{\sigma}$ is symmetric with respect to $k/N=1/2$. The above results on k_c and k_{max} can be verified in the figure.

Let us briefly discuss the relevance of our results on the spontaneous energy localization process. It has been already shown that the modulational instability is the fundamental mechanism for spontaneous generation of the discrete breathers out of a small initial perturbation on the ZBM [3,4,8,16]. As pointed out in Ref. [4], more strongly localized breathers appear for smaller k_{max} because $N/2-k_{max}$ can be regarded as an average wave number of amplitude modulation of the ZBM. Therefore, according to the above results, it is expected that in the high energy region more strongly localized breathers emerge for larger θ_{2m} if the order of potential is fixed. In addition, it is expected that more strongly localized breathers emerge for larger m case in the high energy region, provided that $\theta_{2m}=0$. These predictions are confirmed by numerical experiments. We note that in general the localization features, which are expected from our stability analysis considering only the highest order terms in the potential, hold only in the high energy region. When the energy is not sufficiently large, the effect of lower order terms in the potential might appear and significantly modify the above expected localization features. For instance, it is shown in Ref. [8] that a cubic power correction to the quartic FPU potential weakens localization.

V. CONCLUSIONS

We studied the modulational instability of the ZBM in nonlinear lattices with polynomial on-site and interaction potentials. We obtained an exact expression for the normalized instability growth rate $\tilde{\sigma}(k)$ in the high energy limit. The critical wave number k_c for unstable perturbations and the most unstable wave number k_{max} were determined. In addition, the energy scaling law of the instability growth rate, Eq. (39), was derived. Relevance of the present results on the energy localization state induced by the modulational instability was also discussed.

In the present paper, for simplicity, we assumed that both of the on-site potential U and the interaction potential V include only even order terms. Finally, we remark that the present results hold also for an interaction potential V including odd order terms, provided that the highest order term of V is of an even order.

ACKNOWLEDGMENTS

The author would like to thank the members of NTT Communication Science Laboratories for their continual encouragement.

[1] E. Fermi, J. Pasta, and S. Ulam, *Collected Papers of E. Fermi*, edited by E. Segré (University of Chicago Press, Chicago, 1965).

[2] V. M. Burlakov, S. A. Kiselev, and V. I. Rupasov, Phys. Lett. A **147**, 130 (1990).

[3] T. Cretegny, T. Dauxois, S. Ruffo, and A. Torcini, Physica D **121**, 109 (1998).

[4] Y. A. Kosevich and S. Lepri, Phys. Rev. B **61**, 299 (2000).

[5] S. Takeno, K. Kisoda, and A. J. Sievers, Prog. Theor. Phys. Suppl. **94**, 242 (1988).

[6] K. Ullmann, A. J. Lichtenberg, and G. Corso, Phys. Rev. E **61**, 2471 (2000).
[7] N. Budinsky and T. Bountis, Physica D **8**, 445 (1983).
[8] K. W. Sandusky and J. B. Page, Phys. Rev. B **50**, 866 (1994).
[9] P. Poggi and S. Ruffo, Physica D **103**, 251 (1997).
[10] T. Dauxois, S. Ruffo, and A. Torcini, Phys. Rev. E **56**, R6229 (1997).
[11] T. Dauxois, S. Ruffo, and A. Torcini, J. Phys. IV **8**, 147 (1998).
[12] K. Yoshimura, Phys. Rev. E **62**, 6447 (2000).
[13] G. M. Chechin, N. V. Novikova, and A. A. Abramenko, Physica D **166**, 208 (2002).
[14] G. M. Chechin, D. S. Ryabov, and K. G. Zhukov, nlin.PS/0403040.
[15] Y. S. Kivshar and M. Peyrard, Phys. Rev. A **46**, 3198 (1992).
[16] I. Daumont, T. Dauxois, and M. Peyrard, Nonlinearity **10**, 617 (1997).
[17] H. Yoshida, Physica D **29**, 128 (1987).
[18] H. Yoshida, Commun. Math. Phys. **116** 529 (1988).
[19] J. Plemelj, *Problems in the Sense of Riemann and Klein* (Interscience, New York, 1962).